Repositorio Institucional de la Universidad Autónoma de Madrid

https://repositorio.uam.es

Esta es la **versión de autor** del artículo publicado en:
This is an **author produced version** of a paper published in:

Electrochimica Acta 298 (2019): 950-959

DOI: https://doi.org/10.1016/j.electacta.2018.12.106

Copyright: © 2018 Elsevier Ltd. All rights reserved.

El acceso a la versión del editor puede requerir la suscripción del recurso

Access to the published version may require subscription

Spectroelectrochemical *operando* method for monitoring a phenothiazine electrografting process on amide functionalized C-nanodots/Au hybrid electrodes

Emiliano Martínez-Periñán[1,3], Iria Bravo[1,3], Mónica Mediavilla[1], Mónica Revenga-Parra[1,2,3], Eva Mateo-Martí[4], Félix Pariente[1,2], Encarnación Lorenzo*[1,2,3]

[1]-Departamento de Química Analítica y Análisis Instrumental and [2]-Institute for Advanced Research in Chemical Sciences (IAdChem) Universidad Autónoma de Madrid, 28049, Madrid, Spain.

[3]-Instituto Madrileño de Estudios Avanzados en Nanociencia (IMDEA-Nanociencia), Campus de Cantoblanco, 28049 Madrid, Spain.

[4]-Centro de Astrobiología (CSIC-INTA), Ctra. Ajalvir, Km. 4, 28850, Torrejón de Ardoz, Madrid, Spain.

Keywords

Spectroelectrochemistry, Azure A, electrografting, diazonium salt, carbon nanodots.

Abstract

Phenothiazine derivatives are extensively explored dye molecules, which present interesting electrochemical and optical properties. In recent years, the possibility of transforming some phenothiazines in their aryl diazonium salt derivatives has been proved, what allows them to be electrochemically reduced and electrografted onto conductive surfaces. This is a smart way to modify these surfaces and enable them with

This manuscript version is made available under the CC-BY-NC-ND 4.0 license http://creativecommons.org/licenses/by-nc-nd/4.0/

specific functionalities. In order to better comprehend the electrografting process and consequently have a higher control of it, in this work we have carried out an exhaustive study by *operando* UV-Vis spectroelectrochemistry of the electrografting of a phenothiazine aryl diazonium salt onto amide carbon nanodots. As a model of phenothiazine dye we have chosen Azure A. The electrografting onto carbon nanodots has been stablished by comparison with the results obtained on bare gold electrodes in this novel study. The presence of carbon dots improves the reversibility of the electrochemical process as derived from the results obtained by *operando* UV-Vis spectroelectrochemistry. In addition, to asses that the electrochemical process studied corresponds to the electrografting, the results have been compared to the those obtained for the simple Azure A adsorption. This study shows the advantages of obtaining simultaneously the electrochemical and the spectroscopic evolution of an electron-transfer process in a single experiment, in a particular electrochemical reaction. This work could be the starting point for the study of the electrografting on other nanomaterials.

1. Introduction

The use of aryl diazonium salts for electrode modification has shown great potential in different applications like biosensors [1], DNA sensors [2], immunosensors [3], antifouling [4], corrosion [5], proton exchange membrane fuel cells [6], electrocatalysis [7-10], etc. Pinson et al. [11] were the first to report that aryl diazonium salts could be reductively grafted onto the surface of carbon electrodes to yield covalently attached layers. Electrochemical reduction generates aryl radicals that reacts with the electrode surface to produce a covalent C-C bond [12]. The generation of a covalent bond on gold electrodes (C-Au) has also been demonstrated in the literature [13-15].

This manuscript version is made available under the CC-BY-NC-ND 4.0 license http://creativecommons.org/licenses/by-nc-nd/4.0/

The wide use of this methodology, commonly named electrografting, makes it interesting to study it in depth using techniques that provide different and complementary information. Recent research has tended to use the named o*perando* techniques. The development of *operando* methodologies, which operate under potential control, can help identify reaction products and offer great insights on electrochemical processes. They allow the electrode surface characterization while the electrochemical process is happening. Different techniques have been coupled with electrochemistry, like scanning probe microscopy [16, 17], Raman spectroscopy [18-20], UV-Vis [21], X-ray diffraction [22], transmission electron microscopy [23], etc. In particular, spectroelectrochemistry has been used to study complex reaction mechanisms [24-26]. It proves to be a powerful tool in electrode process microenvironment examination, including the diffusion layer and the electrode surface [27].

Phenothiazine derivatives belong to an extensively explored group of dyes due to their electrochemical and optical properties. Some phenothiazines have been used as redox mediators for biosensing [28-30], solar batteries [31, 32] or fuel cells [33]. Some of them present an aromatic amine in their structure, which can be diazotized to generate a diazonium salt and then electrografted onto different materials. Among them, in this work we have focused our attention on Azure A (AA). Electrografting of this phenothiazine has been previously reported onto carbon [34, 35], gold and graphene modified gold electrodes [36]. These modified electrodes have been employed as NADH electrocatalysts.

The use of carbon nanomaterials as modifiers has resulted on some advantages in the electrocatalytic properties of the resulting modified electrodes [36]. This fact makes it really interesting to analyze in depth the mechanism of modification of functionalized carbon based nanomaterials. Among them, great advances have been demonstrated with

This manuscript version is made available under the CC-BY-NC-ND 4.0 license http://creativecommons.org/licenses/by-nc-nd/4.0/

carbon nanotubes and graphene, and nowadays the use of other carbon allotropes, such as carbon nanodots, is being studied, since they present important benefits, providing similar advantages to carbon nanotubes and graphene, but being synthesized by simpler routes [37]. This nanomaterial is of particular interest in electrochemistry, since it has inherent benefits compared to other carbon-based materials [37, 38], such as its edge-abundant morphology that conveys significant electrocatalytic activity [39] and the possibility of nanostructuring the electrode surface, generating a hybrid material interface. They usually present different surface functional groups, which define their optical properties [40] and also their chemical reactivity, allowing the nanomaterial to be chemically modified with a tailored reactive and endowing it with additional properties. These features make the study of the modification process by operando techniques [41] important.

In this work we have focused our attention on the spectroelectrochemical study (UV-Vis) of the electrografting process of AA diazonium salt by electrochemical reduction at amide functionalized carbon nanodots/gold hybrid electrodes and bare gold electrodes. It has been previously demonstrated that the organic film generated during the electrografting process is more stable and higher recoveries are obtained when carbon nanomaterials are part of the electrode surface [36]. However, although electrochemical techniques can provide evidence about the reaction mechanisms and potential reaction intermediates, a full description and analysis often requires the use of complementary techniques; especially spectroscopic and structural. Hence, in the present work we have analyzed the main changes in the spectroelectrochemical behavior during the electrografting of AA onto a new carbon-based nanomaterial and a metallic surface. Complementary data have been obtained from electrochemical quartz crystal microbalance and X-ray photoelectron spectroscopy analysis.

This manuscript version is made available under the CC-BY-NC-ND 4.0 license http://creativecommons.org/licenses/by-nc-nd/4.0/

2. Experimental

2.1. Reagents and Apparatus

Azure A chloride, sodium nitrite ($NaNO_2$), ethyleneglycol bis-(2-aminoethyl ether)-N,N,N',N'-tetraacetic acid (EGTA) and tris(hydroxymethyl)aminomethane (TRIS) were obtained from Sigma-Aldrich Chemical Co. and used as received. 37% Hydrochloric acid (HCl) was obtained from Scharlau. Water was purified with a Millipore Milli-Q system.

Carbon nanodots rich in amide groups (amd-CDs) have been synthesized by thermal carbonization using EGTA as the carbon source and TRIS as the surface passivation agent according to the method reported by Ahmed et al [42] and fully characterized in previous group works [39, 43]. From this preparation, a suspension containing 1.51 mg ml^{-1} of this nanomaterial was prepared and used for electrode modification.

Integrated screen-printed gold electrodes (SPAuE) (4 mm diameter, Ref 220BT) from Metrohm DropSens S. L. (Oviedo, Spain) including a silver pseudoreference electrode and a gold counter electrode were used. The electrodes were connected using a SPE connector (Metrohm DropSens S. L.) as interface.

For Electrochemical Quartz Crystal Microbalance measurements, the SRS QCM200 Quartz Crystal Microbalance from SRS Instruments (Sunnyvale, CA., USA) was coupled with an Autolab PGSTAT 30 potentiostat using NOVA 1.11 software package. Electrochemical measurements were performed in a single-compartment home-made electrochemical cell where 5 MHz AT-Cut Gold-Chromium (Au-Cr) coated crystals (1 inch diameter) from SRS Instruments were used as working electrode, Pt wire (1 mm diameter) as counter electrode and Ag/AgCl as reference electrode. This technique is an extremely sensitive mass sensor capable of providing mass per unit area by measuring

This manuscript version is made available under the CC-BY-NC-ND 4.0 license http://creativecommons.org/licenses/by-nc-nd/4.0/

the change in frequency of the gold quartz crystal resonator using the Sauerbrey's equation:

$\Delta m = -C_f \cdot \Delta f$

where Δm is the mass change (ng cm^{-2}), C_f (17.7 ng $Hz^{-1}cm^{-2}$) is a proportional constant for 5.0 MHz crystals used in this study, and Δf is the frequency change (in Hertz). Increases in mass cause decrease in frequency and *vice versa*.

X-ray Photoelectron Spectroscopy (XPS) analysis of the samples was carried out with a Phoibos 150 MCD spectrometer equipped with hemispherical electron analyzer, and using a Al Kα X-ray source (1486.7 eV). The base pressure in the ultra high vacuum chamber was 2 x 10^{-9} mbar, and the experiments were carried out a room temperature. A 30 eV pass energy was applied for taking the overview sample, whereas 20 eV pass energy was applied for the analysis of the following core level spectra: O 1s, C 1s, N 1s. XPS spectra regions were fitted and deconvoluted using the fitt-xps software, calibration was done against the Au 4f 84.0 eV. For XPS gold AFM plates (12 mm × 12 mm, Arrandee™ Supplies, Germany) were modified and used as working electrode. A homemade Teflon electrochemical cell with an active window of 0.6 cm^2 was used, in which the Au planar electrodes were sandwiched between an O-ring in the Teflon body and the base.

UV–Vis absorption spectra were recorded on a double beam PharmaSpec UV-1700 series Shimadzu spectrophotometer operating from 200 nm to 800 nm.

Spectroelectrochemical measurements were carried out using an Spelec system (Metrohm DropSens S. L.) using the DROPVIEW SPELEC Software. This system is equipped with a Bipotentiostat/Galvanostat (± 4 V DC potential range, ± 40 mA maximum measurable current) and a Spectrometer wavelength range: 200-900 nm. The experiments were

This manuscript version is made available under the CC-BY-NC-ND 4.0 license http://creativecommons.org/licenses/by-nc-nd/4.0/

carried out in reflection mode, using a Teflon reflection cell (Metrohm DropSens S. L.). Electrochemical studies were carried out with the same equipment using only the potentiostat mode and placing a drop of 100 μL of the corresponding solution onto the SPAuE.

2.2. Electrode modification with amd-CDs

amd-CDs modified electrodes were prepared by dropcasting aliquots of the amd-CDs solution onto the working electrode (SPAuE or Au AFM plates) with a micropipette. The electrodes were modified with 120 μg cm^{-2} or 240 μg cm^{-2} of amd-CDs. After 30 minutes, the solvent completely evaporated (at room temperature) and the modified electrodes were then ready for use.

2.3. Electrografting of AA diazonium salt

Diazotation of AA was performed in an ice bath by mixture of 1.0 mL of 20.0 mM AA (prepared in 0.2 M HCl) and 1.0 mL of 20.0 mM $NaNO_2$ in water. The mixture was kept at 4 ºC for 10 min and was then ready for use in electrode modification. The electrografting was made by immersing the appropriate electrode in the AA diazonium salt (10 mM) solution and cycling the potential between +0.5 V and −0.5 V at 0.10 V s^{-1} to electrochemically reduce the *in situ* generated AA diazonium salt as previously described [33]. Finally, the modified electrodes were rinsed with water and the electrochemical measurements were carried out in 0.1 M HCl.

2.4. UV-Vis characterization of the interaction of AA and AA diazonium salt with amd-CDs

For UV-vis titrations the AA or AA diazonium salt concentration was fixed at 62.5 μM and amd-CDs concentration was varied from 0.1 to 8.5 μg mL^{-1} in 0.1 M HCl.

This manuscript version is made available under the CC-BY-NC-ND 4.0 license http://creativecommons.org/licenses/by-nc-nd/4.0/

2.5. Characterization of the electrografting process by operando UV-Vis spectroelectrochemistry

The AA diazonium salt solution was diluted from 10 mM to 62.5 µM in order to measure at the same time the electrochemical and UV-Vis spectroscopy response without saturating the optical detector (high concentrations of high molar extinction coefficient compounds impede the proper measure without high level of noise). The potential was cycled between +0.40 V and −0.05 V at 0.01 V s^{-1} to electrochemically reduce the AA diazonium salt.

As a control, the electrodes were immersed in 62.5 µM non-diazotized AA and the same electrochemical conditions above described were applied.

3. Results and discussion

3.1. Electrografting of AA diazonium salt

A freshly prepared AA diazonium salt solution was employed for AA electrografting onto amd-CDs modified SPAuE (amd-CDs/SPAuEs) and SPAuE (as control) by electrochemical reduction. The obtained cyclic voltammograms (CV) are shown in Figure 1(A, B, C). In the first cathodic scan, a small peak at +0.30 V can be observed, ascribed to a non-specific adsorption, as well as a peak at +0.06 V and a small shoulder at −0.05 V, which are ascribed to the reduction of the phenothiazine and the aryl diazonium group, respectively. The first reverse scan shows only one oxidation process with a well-defined peak at +0.15 V ascribed to the oxidation of the generated reduced phenothiazine (AA_{red}). In the following cathodic scans, the peak at +0.30 V disappears and the peak current associated with the reduction of the cationic dye decreases significantly, while the anodic

This manuscript version is made available under the CC-BY-NC-ND 4.0 license http://creativecommons.org/licenses/by-nc-nd/4.0/

peak increases slightly. A similar behavior was observed in the control experiments with bare SPAuEs, except for the fact that a higher intensity is observed on the first cathodic peak. However, if after several cycles the electrode is removed from the cell, rinsed with water and placed in 0.1 M HCl, the electrode response ascribed to the oxidation and reduction of the immobilized AA centered at +0.25 V is higher for amd-CDs/SPAuEs (see Figures 1D, E and F, black lines). This effect agrees well with the increase of the specific surface area caused by the presence of amd-CDs on the electrode surface. In addition, it has been described that carbon is a better material than gold to carry out the electrografting [44, 45].

To asses that the above described voltammograms are due to the electrografting of AA and not to other processes, like phenotiazine adsorption, similar voltammetric experiments were carried out under the same conditions but using AA without previous diazotization. Figure 1D, E and F (red line) shows the response of the resulting modified electrode in 0.1 M HCl containing no AA. As can be seen, no redox response at +0.25 V for electrografted species is observed. These results indicate that in the absence of electrografting, the immobilization of AA by adsorption or electropolymerization can be considered negligible.

Figure 1

The process was also analyzed by electrochemical quartz crystal microbalance (EQCM) in order to estimate the amount of phenothiazine grafted on the electrode surface. The gold quartz crystal resonator, either modified with amd-CDs or without modification, was used as a working electrode, providing simultaneously real-time monitoring of mass changes onto the gold electrode surface associated to the electrografting event. After temperature, frequency and resistance had stabilized, cyclic voltammetry, under the same experimental conditions as those described above, was performed. Cyclic

This manuscript version is made available under the CC-BY-NC-ND 4.0 license http://creativecommons.org/licenses/by-nc-nd/4.0/

voltammograms of Azure A electrografting as well as the resulting frequency changes as a function of successive potential scans were recorded (see Figure S1 of supporting information). Either at bare or amd-CDs modified gold surfaces, the first scan of the cyclic voltammograms shows the expected peak ascribed to the reduction of the diazo group formed after the diazotation reaction. On the subsequent scans, the corresponding reduction and oxidation wave decreases as a consequence of the electrografting process. Concomitant with these processes, as the scan goes to reduction potentials, a decrease in the resonant frequency of gold resonator occurs for every cycle in agreement with the formation of an Azure A grafted film. Therefore, from the Δf and using equation (1), assuming that the frequency decrease is mainly due to the change in mass arising from the grafting of molecules, the amount of Azure A electrografted was calculated to be 0.92 and 0.39 μg cm^{-2} for amd-CDs modified and bare gold quartz crystal resonator, respectively. These results agree well with the electrode response obtained after several electrografting cycles and confirm that the presence of amd-CDs gives rise to an increase of the electrografted material.

XPS experiments were also carried out in order to confirm the electrografting process onto amd-CDs/Au electrodes and Au electrodes. Figure 2 shows the C 1s spectrum region obtained from the analysis of amd-CDs/ Au electrodes (Figure 2A) and Au electrodes (Figure 2B) modified with AA by the above described electrografting process. As can be clearly observed when comparing spectra A and B, in the case of amd-CDs/Au electrodes the carbon components at 286.5 eV and 288.5 eV, assigned to C-C=0 and C=N functional groups respectively [46-49], increase their signal intensity with respect to the component at 285.0 eV assigned to (C-C and C-H bond) [46,47]. This is a consequence of the higher amount of AA attached to the electrode surface when amd-CDs are present.

This manuscript version is made available under the CC-BY-NC-ND 4.0 license http://creativecommons.org/licenses/by-nc-nd/4.0/

It is also worth to mention that the S 2p region (see Figure 2D) shows a detectable signal of S only when the electrografting of AA is carried out on amd-CDs/Au electrodes, therefore, when the amount of AA on the electrode is large enough to be detected.

We have also corroborated by XPS that the main process for AA electrode modification is electrografting by comparing the spectra obtained from the analysis of amd-CDs/Au electrodes modified with electrografted or just adsorbed Azure A (Figure 2C). The C 1s region shows a higher intensity in the case of the electrografting (Figure 2A) compared to adsorption (Figure 2C), and the deconvolution of the C 1s region shows a different number of components for each case. In particular, the band at 289.8 eV associated with amide functional groups, only appears in the case of adsorbed AA [46,47]. This band, which comes from amide groups of amd-CDs, does not appear when AA is electrografted on them. Although largely speculative by our part, based on these results, we believe that this is due to the attack of the AA aryl radical, formed during the electrochemical reduction of AA diazonium salt, to the carbon of the amide causing the release of an ammonium cation.

Furthermore, the N 1s region (Figure 2E) of AA modified amd-CDs/Au electrodes shows a higher intensity in the case of the electrografted AA compared to the just adsorbed one. As both surfaces have nanodots (amide functionality) the increase of the intensity from the nitrogen signal is only due to the main amount of AA on the electrode.

Figure 2

3.2. UV-Vis study of interaction between AA and AA Diazonium salt with amd-CDs

This manuscript version is made available under the CC-BY-NC-ND 4.0 license http://creativecommons.org/licenses/by-nc-nd/4.0/

The interaction between AA and amd-CDs was studied by UV-Vis spectrophotometry. Spectra of AA and AA diazonium salt were recorded in a 62.5 µM concentration in acidic media. Both spectra show a band at 635 nm, at which the absorbance for AA is higher than that for AA diazonium salt. A band at 446 nm can be also observed in the case of the diazonium salt, which can be attributed to the diazonium group.

Figure 3.

In the presence of increasing concentrations of amd-CDs, a hyperchromic effect in the 635 nm band is observed for both AA forms. The effect is more evident in the case of the non-diazotized form, what suggests that amd-CDs interact preferably with this form, probably due to the presence of amine groups.

3.3. Operando spectroelectrochemical studies

In order to better understand the above described electrografting process, we decided to perform an *operando* UV-Vis spectroelectrochemical study. The combination of *operando* spectrophotometric and electrochemical techniques to analyze the surface process involving dyes provides a valuable information that would not be obtained by performing both techniques separately.

3.3.1. Non-diazotized AA salt solution

As in the above described results, and as a comparison, at a first step the electrochemical behavior of a non-diazotized dye solution (62.5 µM AA in 0.1 M HCl) at the 3 different electrochemical platforms developed was studied. Figure 4A, B and C shows the first scan of the cyclic voltammetry obtained with SPAuE, 120 µg cm^{-2} amd-CDs/SPAuE and 240 µg cm^{-2} amd-CDs/SPAuE, respectively. In all cases, a redox couple at E^0 = +0.07 V, due to the oxidation/reduction of the phenothiazine, appears. The cathodic peak presents

This manuscript version is made available under the CC-BY-NC-ND 4.0 license http://creativecommons.org/licenses/by-nc-nd/4.0/

two contributions at +0.08 V and +0.04 V. The first one is related to the diffusion of AA process and the second one to its adsorption. This fact is confirmed by scan rate study, since the peak current of the first process increases linearly with the square root of the scan rate, but for the second process (at +0.04V) the peak current increases linearly on increasing the scan rate up to 100 mVs^{-1} (see figure S2 of Supporting Information).

The adsorption process contributes in a higher degree than the diffusional one when amd-CDs are present on the electrode surface. Like in the initial study, an increase of amd-CDs amount implies a decrease in the current intensity of the redox pair ascribed to the reduction of the oxidized form of AA (AA_{ox}) and the subsequent oxidation of the generated reduced form (AA_{red}). It clearly shows the less conductive nature of the carbon nanomaterial compared to the bare gold electrode. Besides, the number of faradaic processes and the redox peak formal potentials are the same regardless the electrodic platform employed.

The spectra evolution of the different electrochemical platforms during the above-mentioned redox process is shown in Figure 4D, E and F. In all the cases, a decrease in the absorbance of a wide band with two differentiated peaks at 590 nm and 630 nm is observed. This phenomenon is related to the decrease in the main band of the AA spectrum (Figure 3A), corresponding to the AA_{ox} species. As the AA_{ox} is electrochemically reduced during the process at +0.04 V, the main absorbance band decreases, since AA_{red} absorbs at a different wavelength. As the cathodic scan potential goes further, the absorbance of the main band (590 nm and 630 nm) decreases, even during the anodic scan when the potentials are below the oxidation process. Once the oxidation process begins, the variation of the absorbance starts growing, but the starting absorbance value is not entirely recovered, pointing out that the process is not totally reversible.

This manuscript version is made available under the CC-BY-NC-ND 4.0 license http://creativecommons.org/licenses/by-nc-nd/4.0/

In the presence of amd-CDs, the main change of absorbance during the above described electrochemical process follows a similar trend, but the magnitude of the absorbance change decreases with the amount of amd-CDs. This fact is associated with the lower amount of AA_{ox} reduced during the electrochemical process as evidenced in the corresponding cyclic voltammograms.

It is worth to note that in the case of amd-CDs modified electrode surfaces, the absorbance at the main band (590 nm and 630 nm) is fully recovered, reaching the initial values after the complete cyclic voltammetry scan, what indicates a better electron transfer communication between the AA_{red} species and the electrode surface when amd-CDs are used. This behavior is different to that observed in a previous work where carboxylated carbon nanodots (COOH-CDs) were used [50]. In that case the absorbance variation at 590 nm and 630 nm is higher when COOH-CDs are present compared to the bare SPAuE and the initial absorbance is not completely recovered once the potential scan is finished. Hence, the different behavior observed is a clear evidence of the influence of functional groups present on CDs on the electrochemical response of the platform for a certain electrochemical process, as demonstrated by *operando* UV-Vis spectroelectrochemical analysis.

Figure 4.

3.3.2. AA diazonium salt solution

The electrografting process was studied following the same *operando* method, but using in this case a 62.5 µM solution of AA diazonium salt in 0.1 M HCl. The cyclic voltammograms show (Figure 5A, B, C), during the cathodic scan, a first peak around +0.14 V corresponding to the reduction of the phenothiazine AA_{ox} to AA_{red} and a second peak at +0.05 V associated with the electrografting process of the aryl diazonium salt. The same electrochemical behavior has been observed at the three electrochemical

This manuscript version is made available under the CC-BY-NC-ND 4.0 license http://creativecommons.org/licenses/by-nc-nd/4.0/

platforms under study. It is also remarkable that the current intensity decreases slightly with higher amounts of amd-CDs on the electrode surface, but the magnitude of this decrease is not as big as in the case of non-diazotized AA, which means that the electron transfer with amd-CDs is better in the case of AA diazonium salt than for the non-diazotized AA molecule.

The absorbance variations during the first potential scan are shown in Figure 5D, E and F. In all cases a band at 630 nm appears, which increases as the two cathodic processes take place. This band is ascribed to the reduction of the aryl diazonium salt and the generation of a species similar to AA covalently attached to the electrode surface (gold in SPAuE or a mixture of bonds with gold and carbon in the case of amd-CDs/SPAuE hybrid electrodes).

The electrografted AA species is the responsible for the absorbance increase at 630 nm. Concomitant, the band at 430 nm, associated with the diazo group (Figure 3A black spectrum), decreases during the cathodic process at + 0.05 V, which is consistent with the conversion of AA diazonium salt into electrografted AA. The band at 550 nm is associated with the phenothiazine reduction/oxidation process. It decreases as the potential moves to values below +0.14 V, since at these potentials the reduced dye form (AA_{red}) is the prevalent one. At higher potentials than +0.14 V, the absorbance at 550 nm recovers its initial value, since the dye is in its oxidized form, AA_{ox}. Even a slight absorbance increase of the band at 550 nm is observed at the end of the cyclic voltammogram. This is a consequence of the generation of AA_{ox} electrografted from the solution of AA_{ox} diazonium salt, due to the higher absorbance of AA_{ox} at this wavelength when compared to the AA_{ox} diazonium salt. It is worth to note that in this case, in a similar way to the previous case for non-diazotized AA, there are some differences in the electrografting process when compared to the observed when COOH-CDs [50] are used

This manuscript version is made available under the CC-BY-NC-ND 4.0 license http://creativecommons.org/licenses/by-nc-nd/4.0/

instead of amd-CDs. The presence of COOH-CDs causes an increase in both the peak current and the absorbance variation compared to the bare SPAuE. However, the behavior for amd-CDs is just the opposite. This observation shows once again the potential applicability of *operando* spectroelectrochemistry to obtain information about complex electrochemical processes, in particular, in the present work to evidence how different surface functional groups present on the C based nanomaterial could affect electrochemical processes.

Figure 5.

3.3.3. Spectroelectrochemical data analysis

With the aim of deepening in the study of the influence of the presence of amd-CDs in the electrografting process and to stablish the differences with the simple adsorption, we have focused now our attention on the spectroelectrochemical data obtained for the two processes at SPAuE and amd-CDs/SPAuE during the first five scans.

Figure 6 shows the absorbance variation at a specific wavelength (440, 550 and 630 nm) *versus* the potential applied to the bare SPAuE (Voltabsorptogram) immersed in AA (red line) or AA diazonium salt (black line) solutions. At 440 nm (Figure 6A) it can be clearly observed no significant variation of the absorbance of the system in the case of AA (adsorption process), whereas in the case of AA diazonium salt (electrografting process) the absorbance decreases upon consecutive potential scans. This fact is consistent with the decrease of the diazonium group's band absorbance (440 nm), as the AA diazonium salt is electrografted on the gold surface during the successive scans, consuming the diazonium group.

The analysis of the first scan voltabsorptogram derivative at 440 nm (Figure 6D) shows a non-reversible peak at +0.07 V, exactly at the same potential of the cathodic peak in the

This manuscript version is made available under the CC-BY-NC-ND 4.0 license http://creativecommons.org/licenses/by-nc-nd/4.0/

cyclic voltammogram, what confirms that the absorbance variation at 440 nm is due to this electrochemical process. No peaks are present in the voltabsorptogram derivative in the anodic scan, indicating that the process becomes irreversible when the AA diazonium salt is electrografted on the electrode, and a covalent bond between the phenothiazine and the electrode surface is stablished.

At 550 nm (Figure 6B) the absorbance decreases at potentials lower than +0.14 V, either during the electrografting process or the simple adsorption of AA molecule. In the case of electrografting (black line), the absorbance recovers its original value at the end of the anodic scan. However, in the case of the adsorption process the absorbance values do not recover at all the original values, what causes an absorbance decrease along the potential scans. This behavior suggests that the redox process is not completely reversible, and not all the AA_{ox} molecules reduced during the cathodic scan are oxidized in the reverse anodic scan. For both processes, the voltabsorptogram derivative presents an identical shape to the cyclic voltammogram, what means that the absorbance variation is related to the electrochemical process of reduction of AA_{ox} and oxidation of AA_{red} generated during the reverse scan.

The absorbance variation at 630 nm (Figure 6C) shows a clear difference between the case of the electrografting and the adsorption process. In the case of electrografting, the absorbance increases during the successive potential scans, whereas in the adsorption process the absorbance decreases. In both cases the voltabsorptogram derivatives (Figure 6F) present an anodic and a cathodic peak at the same potential of the cyclic voltammogram, what clearly shows the correlation between the absorbance variation and the electrochemical processes happening on the electrode surface during the potential scan.

Figure 6.

This manuscript version is made available under the CC-BY-NC-ND 4.0 license http://creativecommons.org/licenses/by-nc-nd/4.0/

The voltabsorptograms and voltabsorptogram derivatives analysis for 120 μg cm^{-2} amd-CDs/SPAuE is shown in Figure 7. At 440 nm, a slight increase of absorbance over time can be observed in the case of the adsorption process (Figure 7A red line). The absence of peaks in the voltabsorptogram derivative (Figure 7D red line) implies that the absorption change is not related to any electrochemical process. It could be due to the important increase of absorbance observed among 350-400 nm (Figure 5E). Hence, it could be related to the chemical adsorption of AA diazonium salt on amd-CDs or, maybe, as other works suggest [51, 52], it could be a non-electrochemical type of aryl diazonium salts de-diazonation, such as photochemical or chemical (by a reducing surface).

In the case of the electrografting, as was the case at the SPAuE, a little decrease can be seen, smaller than that observed at the bare electrode (Figure 6A black line), in the absorbance band at 440 nm ascribed to the diazonium group (Figure 7A black line). This is what one would expect, since the AA diazonium salt is electrografted on the amd-CDs modified electrode surface during electrochemical process, consuming the diazonium group. The corresponding voltabsorptogram derivative (Figure 7D black line) shows a quasi-reversible peak centered at +0.12 V, near the potential of the cathodic peak in the cyclic voltammogram, what suggests that the absorbance variation at 440 nm is due to the electrografting of AA diazonium salt on amd-CDs/SPAuE.

The absorbance variation at 550 nm (Figure 7B) shows a decrease during the cathodic scan and an increase during the anodic scan, recovering the initial absorbance value at the end of the scan both during the electrografting and the simple adsorption process. This behavior, which is different to the one observed for bare SPAuE, indicates that the presence of amd-CDs promotes the reversibility of the electrochemical reduction/oxidation of phenothiazine group. Carbon nanodots may modify and improve the gold properties resulting in electrodes with new functionalities. The nature of the

This manuscript version is made available under the CC-BY-NC-ND 4.0 license http://creativecommons.org/licenses/by-nc-nd/4.0/

electrode surface has a great contribution not only in the assembly of AA molecules but also in their electrochemical properties. In fact, diazotized molecules show a major affinity for carbon than for gold surfaces [44, 45].

The corresponding voltabsorptogram derivatives (Figure 7E) show a reversible peak, which determines that the absorbance change at 550 nm is related to the electrochemical process happening during the potential scan. The formal potential is slightly different among them, what can be also observed in the corresponding CV, and it is a consequence of using a different molecule (AA or AA diazonium salt), but the electrochemical process involved in both cases is the electrochemical reduction/oxidation of the phenothiazine moiety.

Finally, the absorbance variation at 630 nm is clearly different during the adsorption and the electrografting processes (Figure 7C) and different to that observed at bare SPAuE. For the adsorption process, the absorbance changes during the potential scan but it is totally recovered at the end of the scan. This result implies a better reversibility of the electrochemical process (phenothiazine moiety reduction/oxidation) when amd-CDs are employed. In the case of electrografting the absorbance increases during the successive potential scans. In both cases the voltabsorptogram derivative (Figure 7F) presents a pair of peaks at the same potential of the cyclic voltammogram, what demonstrates the correlation between the absorbance variation and the electrochemical processes taking place along the potential scan.

Figure 7.

4. Conclusion

This manuscript version is made available under the CC-BY-NC-ND 4.0 license http://creativecommons.org/licenses/by-nc-nd/4.0/

In this work, a method for functionalizing carbon nanodots synthesized with enriched peripherical amide groups was developed. Additionally, the ability of these nanomaterials to be immobilized on screen printed gold electrodes and further modified with a phenothiazine by electrografting of AA diazonium salt was tested. Electrochemical process characterization by cyclic voltammetry, electrochemical quartz crystal microbalance, X-ray photoelectron spectroscopy and *operando* spectroelectrochemistry confirms the covalent attachment of the phenothiazine to the immobilized amide rich carbon nanodots and allow us to obtain valuable data to acquire a deeper knowledge of the electrografting process and the role that the peripherical amide groups play on it.

Acknowledgments

Funding from the Spanish Ministerio de Ciencia, Innovación y Universidades (project: CTQ2017-84309-C2-1-R,) and Comunidad Autónoma de Madrid (NANOAVANSENS Program) is acknowledged. IMDEA Nanociencia acknowledges support from the 'Severo Ochoa' Programme for Centres of Excellence in R&D (Ministerio de Ciencia, Innovación y Universidades, Grant SEV-2016-0686). Thank you to S. Gálvez-Martínez for help during XPS measurements.

This manuscript version is made available under the CC-BY-NC-ND 4.0 license http://creativecommons.org/licenses/by-nc-nd/4.0/

References

[1] O. Rüdiger, J.M. Abad, E.C. Hatchikian, V.M. Fernandez, A.L. De Lacey, Oriented Immobilization of Desulfovibrio gigas Hydrogenase onto Carbon Electrodes by Covalent Bonds for Nonmediated Oxidation of H_2, J. Am. Chem. Soc., 127 (2005) 16008-16009.

[2] M. Revenga-Parra, T. García-Mendiola, J. González-Costas, E. González-Romero, A.G. Marín, J.L. Pau, F. Pariente, E. Lorenzo, Simple diazonium chemistry to develop specific gene sensing platforms, Anal. Chim. Acta, 813 (2014) 41-47.

[3] V. Serafín, R.M. Torrente-Rodríguez, A. González-Cortés, P. García de Frutos, M. Sabaté, S. Campuzano, P. Yáñez-Sedeño, J.M. Pingarrón, An electrochemical immunosensor for brain natriuretic peptide prepared with screen-printed carbon electrodes nanostructured with gold nanoparticles grafted through aryl diazonium salt chemistry, Talanta, 179 (2018) 131-138.

[4] M. Parviz, N. Darwish, M.T. Alam, S.G. Parker, S. Ciampi, J.J. Gooding, Investigation of the Antifouling Properties of Phenyl Phosphorylcholine-Based Modified Gold Surfaces, Electroanalysis, 26 (2014) 1471-1480.

[5] A. Chaussé, M.M. Chehimi, N. Karsi, J. Pinson, F. Podvorica, C. Vautrin-Ul, The Electrochemical Reduction of Diazonium Salts on Iron Electrodes. The Formation of Covalently Bonded Organic Layers and Their Effect on Corrosion, Chem. Mater., 14 (2002) 392-400.

[6] Y.R.J. Thomas, A. Benayad, M. Schroder, A. Morin, J. Pauchet, New Method for Super Hydrophobic Treatment of Gas Diffusion Layers for Proton Exchange Membrane Fuel Cells Using Electrochemical Reduction of Diazonium Salts, ACS Appl. Mater. Interfaces, 7 (2015) 15068-15077.

This manuscript version is made available under the CC-BY-NC-ND 4.0 license http://creativecommons.org/licenses/by-nc-nd/4.0/

[7] G. Jürmann, D.J. Schiffrin, K. Tammeveski, The pH-dependence of oxygen reduction on quinone-modified glassy carbon electrodes, Electrochim. Acta, 53 (2007) 390-399.

[8] K. Tammeveski, K. Kontturi, R.J. Nichols, R.J. Potter, D.J. Schiffrin, Surface redox catalysis for O2 reduction on quinone-modified glassy carbon electrodes, J. Electroanal. Chem., 515 (2001) 101-112.

[9] E. Kibena, M. Marandi, V. Sammelselg, K. Tammeveski, B.B.E. Jensen, A.B. Mortensen, M. Lillethorup, M. Kongsfelt, S.U. Pedersen, K. Daasbjerg, Electrochemical Behaviour of HOPG and CVD-Grown Graphene Electrodes Modified with Thick Anthraquinone Films by Diazonium Reduction, Electroanalysis, 26 (2014) 2619-2630.

[10] M. Mooste, E. Kibena-Põldsepp, B.D. Ossonon, D. Bélanger, K. Tammeveski, Oxygen reduction on graphene sheets functionalised by anthraquinone diazonium compound during electrochemical exfoliation of graphite, Electrochim. Acta, 267 (2018) 246-254.

[11] M. Delamar, R. Hitmi, J. Pinson, J.M. Saveant, Covalent modification of carbon surfaces by grafting of functionalized aryl radicals produced from electrochemical reduction of diazonium salts, J. Am. Chem. Soc., 114 (1992) 5883-5884.

[12] C. Combellas, F. Kanoufi, J. Pinson, F.I. Podvorica, Time-of-Flight Secondary Ion Mass Spectroscopy Characterization of the Covalent Bonding between a Carbon Surface and Aryl Groups, Langmuir, 21 (2005) 280-286.

[13] L. Guo, L. Ma, Y. Zhang, X. Cheng, Y. Xu, J. Wang, E. Wang, Z. Peng, Spectroscopic Identification of the Au–C Bond Formation upon Electroreduction of an Aryl Diazonium Salt on Gold, Langmuir, 32 (2016) 11514-11519.

[14] M. Mooste, E. Kibena-Poldsepp, M. Marandi, L. Matisen, V. Sammelselg, K. Tammeveski, Electrochemical properties of gold and glassy carbon electrodes

This manuscript version is made available under the CC-BY-NC-ND 4.0 license http://creativecommons.org/licenses/by-nc-nd/4.0/

electrografted with an anthraquinone diazonium compound using the rotating disc electrode method, RSC Adv., 6 (2016) 40982-40990.

[15] I. Bravo, T. García-Mendiola, M. Revenga-Parra, F. Pariente, E. Lorenzo, Diazonium salt click chemistry based multiwall carbon nanotube electrocatalytic platforms, Sens. Actuators B Chem., 211 (2015) 559-568.

[16] A.A. Gewirth, B.K. Niece, Electrochemical Applications of in Situ Scanning Probe Microscopy, Chem. Rev., 97 (1997) 1129-1162.

[17] K. Itaya, In situ scanning tunneling microscopy in electrolyte solutions, Prog. Surf. Sci., 58 (1998) 121-247.

[18] Y. Deng, L.R.L. Ting, P.H.L. Neo, Y.-J. Zhang, A.A. Peterson, B.S. Yeo, Operando Raman Spectroscopy of Amorphous Molybdenum Sulfide (MoSx) during the Electrochemical Hydrogen Evolution Reaction: Identification of Sulfur Atoms as Catalytically Active Sites for H+ Reduction, ACS Catal., 6 (2016) 7790-7798.

[19] G.G. Rodríguez-Calero, S. Conte, M.A. Lowe, S.E. Burkhardt, J. Gao, J. John, K. Hernández-Burgos, H.D. Abruña, In situ electrochemical characterization of poly-3,4-ethylenedioxythiophene/tetraalkylphenylene diamine films and their potential use in electrochemical energy storage devices, J. Electroanal. Chem., 765 (2016) 65-72.

[20] E. Martínez-Periñán, M. Revenga-Parra, J. Pastore, F. Pariente, F. Zamora, O. Castillo, E. Lorenzo, H.D. Abruña, Operando Methods for the Mechanistic Elucidation of an Electrochemically Driven Structural Transformation, J. Phys. Chem. C, 122 (2018) 12377-12383.

[21] N. González-Diéguez, A. Colina, J. López-Palacios, A. Heras, Spectroelectrochemistry at Screen-Printed Electrodes: Determination of Dopamine, Anal. Chem., 84 (2012) 9146-9153.

This manuscript version is made available under the CC-BY-NC-ND 4.0 license http://creativecommons.org/licenses/by-nc-nd/4.0/

[22] K.E. Silberstein, J.P. Pastore, W. Zhou, R.A. Potash, K. Hernandez-Burgos, E.B. Lobkovsky, H.D. Abruna, Electrochemical lithiation-induced polymorphism of anthraquinone derivatives observed by operando X-ray diffraction, Phys Chem Chem Phys, 17 (2015) 27665-27671.

[23] X.H. Liu, J.Y. Huang, In situ TEM electrochemistry of anode materials in lithium ion batteries, Energy Environ Sci., 4 (2011) 3844-3860.

[24] A. Heras, A. Colina, V. Ruiz, J. López-Palacios, UV-Visible Spectroelectrochemical Detection of Side-Reactions in the Hexacyanoferrate(III)/(II) Electrode Process, Electroanalysis, 15 (2003) 702-708.

[25] C. Fernández-Blanco, Á. Colina, A. Heras, UV/Vis Spectroelectrochemistry as a Tool for Monitoring the Fabrication of Sensors Based on Silver Nanoparticle Modified Electrodes, Sensors, 13 (2013) 5700.

[26] D. Izquierdo, A. Martinez, A. Heras, J. Lopez-Palacios, V. Ruiz, R.A.W. Dryfe, A. Colina, Spatial Scanning Spectroelectrochemistry. Study of the Electrodeposition of Pd Nanoparticles at the Liquid/Liquid Interface, Anal. Chem., 84 (2012) 5723-5730.

[27] Y. Zhai, Z. Zhu, S. Zhou, C. Zhu, S. Dong, Recent advances in spectroelectrochemistry, Nanoscale, (2018).

[28] C. Schlangen, M. Hämmerle, R. Moos, Amperometric enzyme electrodes for the determination of volatile alcohols in the headspace above fruit and vegetable juices, Microchim. Acta, 179 (2012) 115-121.

[29] C. Mousty, S. Cosnier, M. Sanchez-Paniagua Lopez, E. Lopez-Cabarcos, B. Lopez-Ruiz, Rutin Determination at an Amperometric Biosensor, Electroanalysis, 19 (2007) 253-258.

This manuscript version is made available under the CC-BY-NC-ND 4.0 license http://creativecommons.org/licenses/by-nc-nd/4.0/

[30] E. Dempsey, D. Diamond, A. Collier, Development of a biosensor for endocrine disrupting compounds based on tyrosinase entrapped within a poly(thionine) film, Biosens. Bioelectron., 20 (2004) 367-377.

[31] A.K. Jana, Solar cells based on dyes, J Photochem Photobiol A, 132 (2000) 1-17.

[32] K.R. Genwa, A. Kumar, A. Sonel, Photogalvanic solar energy conversion: Study with photosensitizers Toluidine Blue and Malachite Green in presence of NaLS, Appl. Energy, 86 (2009) 1431-1436.

[33] S. Aquino Neto, T.S. Almeida, M.T. Meredith, S.D. Minteer, A.R. De Andrade, Employing Methylene Green Coated Carbon Nanotube Electrodes to Enhance NADH Electrocatalysis for Use in an Ethanol Biofuel Cell, Electroanalysis, 25 (2013) 2394-2402.

[34] B. Doumèche, L.J. Blum, NADH oxidation on screen-printed electrode modified with a new phenothiazine diazonium salt, Electrochem. Commun., 12 (2010) 1398-1402.

[35] M. Revenga-Parra, C. Gómez-Anquela, T. García-Mendiola, E. González, F. Pariente, E. Lorenzo, Grafted Azure A modified electrodes as disposable β-nicotinamide adenine dinucleotide sensors, Anal Chim Acta, 747 (2012) 84-91.

[36] C. Gómez-Anquela, M. Revenga-Parra, J.M. Abad, A.G. Marín, J.L. Pau, F. Pariente, J. Piqueras, E. Lorenzo, Electrografting of N',N'-dimethylphenothiazin-5-ium-3,7-diamine (Azure A) diazonium salt forming electrocatalytic organic films on gold or graphene oxide gold hybrid electrodes, Electrochim. Acta, 116 (2014) 59-68.

[37] H. Li, Z. Kang, Y. Liu, S.-T. Lee, Carbon nanodots: synthesis, properties and applications, J. Mater. Chem., 22 (2012) 24230-24253.

This manuscript version is made available under the CC-BY-NC-ND 4.0 license http://creativecommons.org/licenses/by-nc-nd/4.0/

[38] P. Miao, K. Han, Y. Tang, B. Wang, T. Lin, W. Cheng, Recent advances in carbon nanodots: synthesis, properties and biomedical applications, Nanoscale, 7 (2015) 1586-1595.

[39] E. Martínez-Periñán, I. Bravo, S.J. Rowley-Neale, E. Lorenzo, C.E. Banks, Carbon Nanodots as Electrocatalysts towards the Oxygen Reduction Reaction, Electroanalysis, 30 (2018) 436-444.

[40] S.N. Baker, G.A. Baker, Luminescent Carbon Nanodots: Emergent Nanolights, Angew. Chem. Int. Ed., 49 (2010) 6726-6744.

[41] Z. Zeng, W. Zhang, D.M. Arvapalli, B. Bloom, A. Sheardy, T. Mabe, Y. Liu, Z. Ji, H. Chevva, D.H. Waldeck, J. Wei, A fluorescence-electrochemical study of carbon nanodots (CNDs) in bio- and photoelectronic applications and energy gap investigation, Phys Chem Chem Phys, 19 (2017) 20101-20109.

[42] G.H.G. Ahmed, R.B. Laíño, J.A.G. Calzón, M.E.D. García, Highly fluorescent carbon dots as nanoprobes for sensitive and selective determination of 4-nitrophenol in surface waters, Microchim. Acta, 182 (2015) 51-59.

[43] T. García-Mendiola, I. Bravo, J.M. López-Moreno, F. Pariente, R. Wannemacher, K. Weber, J. Popp, E. Lorenzo, Carbon nanodots based biosensors for gene mutation detection, Sens. Actuators B Chem., 256 (2018) 226-233.

[44] A.L. Gui, G. Liu, M. Chockalingam, G. Le Saux, J.B. Harper, J.J. Gooding, A Comparative Study of Modifying Gold and Carbon Electrode with 4-Sulfophenyl Diazonium Salt, Electroanalysis, 22 (2010) 1283-1289.

[45] X. Zong, N. Kong, J. Liu, W. Yang, M. Cao, J.J. Gooding, The Influence of Graphene on the Electrical Communication Through Organic Layers on Graphite and Gold Electrodes, Electroanalysis, 26 (2014) 84-92.

This manuscript version is made available under the CC-BY-NC-ND 4.0 license http://creativecommons.org/licenses/by-nc-nd/4.0/

[46] J.F.Moulder, W.F.Stickle, P.E.Sobol, K.D. Bomben.) Handbook of X-ray photoelectron spectroscopy. Perkin-Elmer corporation, Physical Electronics Division, Minnesota, United States of America, 1992.

[47] G. Beamson, D. Briggs. The XPS of polymers database; Surface Spectra: Manchester, UK, 2000.

[48] G.P. Lopez, D.G. Castner, B.D. Ratner, Surf. Interface Anal. 17 (1991) 267.

[49] A. Vallée, V. Humblot, C. Méthivier, C.M. Pradier, J. Phys. Chem. C 113 (2009) 9336.

[50] M. Mediavilla, E. Martínez-Periñán, I. Bravo, T. García-Mendiola, M. Revenga-Parra, F. Pariente, E. Lorenzo, Electrochemically driven phenothiazine modification of carbon nanodots, Nano Res., 11 (2018) 6405-6416. https://doi.org/10.1007/s12274-018-2165-y

[51] A. Berisha, C. Combellas, F. Kanoufi, P. Decorse, N. Oturan, J. Médard, M. Seydou, F. Maurel, J. Pinson, Some Theoretical and Experimental Insights on the Mechanistic Routes Leading to the Spontaneous Grafting of Gold Surfaces by Diazonium Salts, Langmuir, 33 (2017) 8730-8738.

[52] S. Bouden, J. Pinson, C. Vautrin-Ul, Electrografting of diazonium salts: A kinetics study, Electrochem. Commun., 81 (2017) 120-123.

This manuscript version is made available under the CC-BY-NC-ND 4.0 license http://creativecommons.org/licenses/by-nc-nd/4.0/

Figures Captions

Figure 1. Cyclic voltammograms of the electrografting of 10.0 mM AA diazonium salt in 0.1 M HCl at SPAuE (A), 120 µg cm^{-2} amd-CDs/SPAuE (B) and 240 µg cm^{-2} amd-CDs/SPAuE (C). Scan rate: 0.10 V s^{-1}. Cyclic voltammograms of SPAuE (D), 120 µg cm^{-2} amd-CDs/SPAuE (E) and 240 µg cm^{-2} amd-CDs/SPAuE (F) electrodes after modification by electrografting (black) or by adsorption (red) in 0.1 M HCl. Scan rate: 0.01 V s^{-1}.

Figure 2. C 1s XPS spectra of electrografted AA/amd-CDs/Au (A), electrografted AA/ Au (B) and just adsorbed AA/amd-CDs/Au (C). S 2p XPS spectra of electrografted AA/amd-CDs/Au (black) and electrografted AA/Au (red). N 1s XPS spectra of electrografted AA/amd-CDs/Au and just adsorbed AA/amd-CDs/Au.

Figure 3. UV-Vis spectra of (A) AA diazonium salt and (B) AA (62.5 µM) in the absence (black line) and in the presence of different concentrations (0.1-8.5 µg mL^{-1}) of amd-CDs (colored lines) in 0.1 M HCl.

Figure 4. Cyclic voltammograms of 62.5 µM AA in 0.1 M HCl at SPAuE (A), 120 µg cm^{-2} amd-CDs/SPAuE (B) and 240 µg cm^{-2} amd-CDs/SPAuE (C). Scan rate: 0.10 V s^{-1}. Corresponding UV-Vis absorbance variation spectra at SPAuE (D), 120 µg cm^{-2} amd-CDs/SPAuE (E) and 240 µg cm^{-2} amd-CDs/SPAuE (F).

This manuscript version is made available under the CC-BY-NC-ND 4.0 license http://creativecommons.org/licenses/by-nc-nd/4.0/

Figure 5. Cyclic voltammograms of the electrografting of 62.5 µM AA diazonium salt in 0.1 M HCl at SPAuE (A), 120 µg cm^{-2} amd-CDs/SPAuE (B) and 240 µg cm^{-2} amd-CDs/SPAuE (C). Scan rate: 0.10 V s^{-1}. Corresponding UV-Vis absorbance variation spectra at SPAuE (D), 120 µg cm^{-2} amd-CDs/SPAuE (E) and 240 µg cm^{-2} amd-CDs/SPAuE (F).

Figure 6. Successive voltabsorptograms (5 scans) at 440 nm (A), 550 nm (B), and 630 nm (C) of the electrografting of 62.5 µM AA diazonium salt (black line) or adsorption of 62.5 µM AA (red line) in 0.1 M HCl at SPAuE. Scan rate: 0.10 V s^{-1}. Corresponding voltabsorptogram derivatives (first scan) at 440 nm (D), 550 nm (E), and 630 nm (F) for AA diazonium salt electrografting (black line) or AA adsorption (red line).

Figure 7. Successive voltabsorptograms (5 scans) at 440 nm (A), 550 nm (B), and 630 nm (C) of the electrografting of 62.5 µM AA diazonium salt (black line) or adsorption of 62.5 µM AA (red line) in 0.1 M HCl at 120 µg cm^{-2}amd-CDs/SPAuE. Scan rate: 0.10 V s^{-1}. Corresponding voltabsorptogram derivatives (first scan) at 440 nm (D), 550 nm (E), and 630 nm (F) for AA diazonium salt electrografting (black line) or AA adsorption (red line).

This manuscript version is made available under the CC-BY-NC-ND 4.0 license http://creativecommons.org/licenses/by-nc-nd/4.0/

Figures

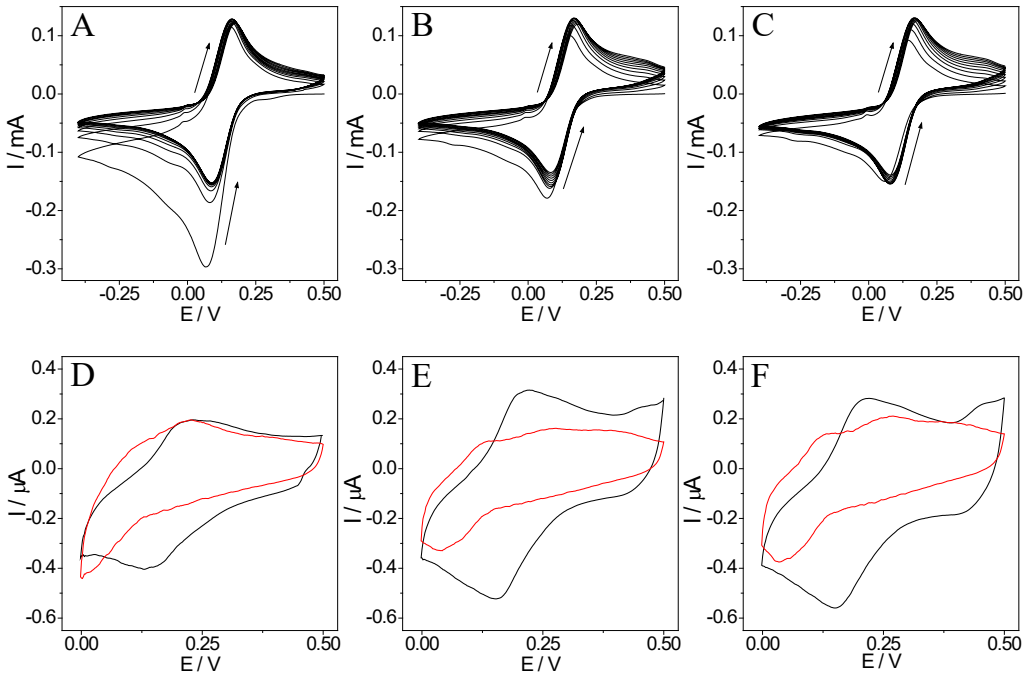

Figure 1.

This manuscript version is made available under the CC-BY-NC-ND 4.0 license http://creativecommons.org/licenses/by-nc-nd/4.0/

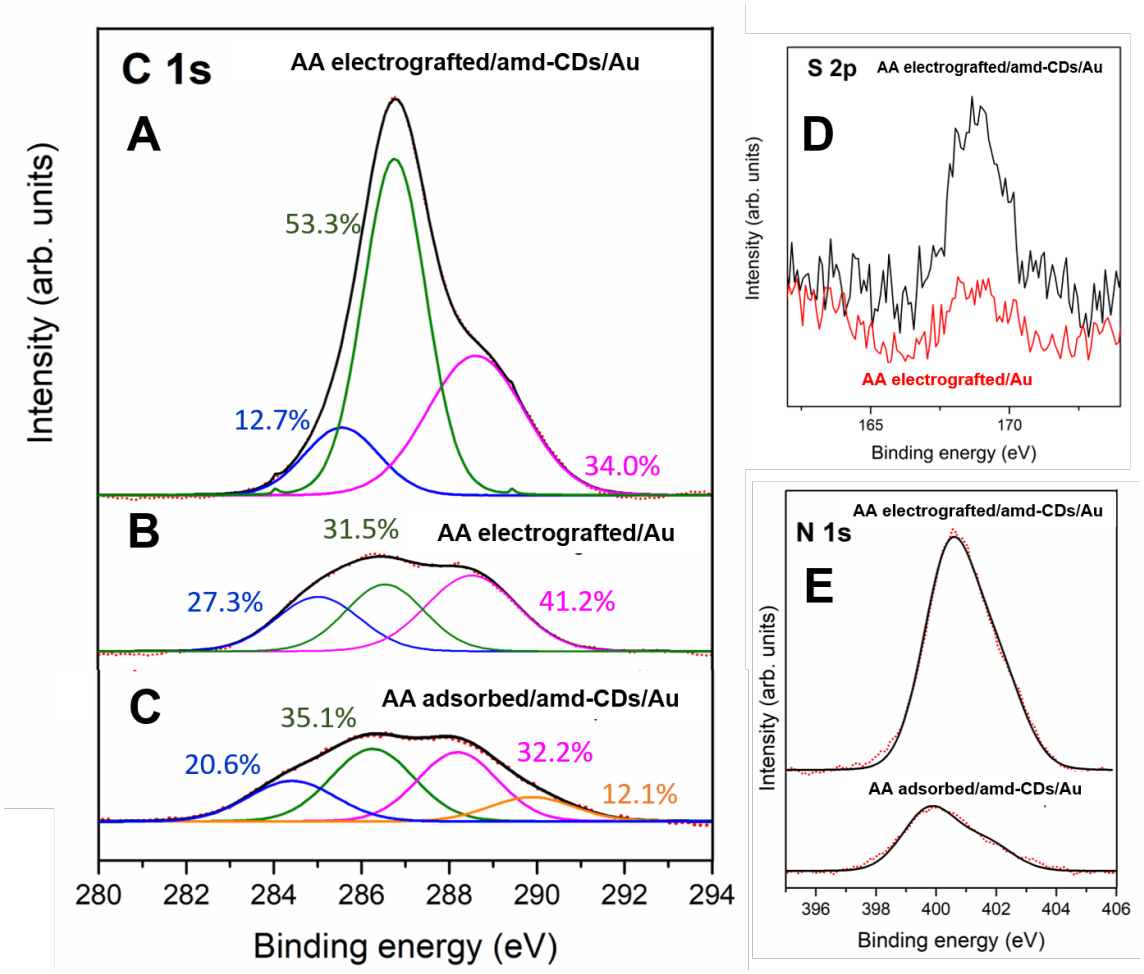

Figure 2.

This manuscript version is made available under the CC-BY-NC-ND 4.0 license http://creativecommons.org/licenses/by-nc-nd/4.0/

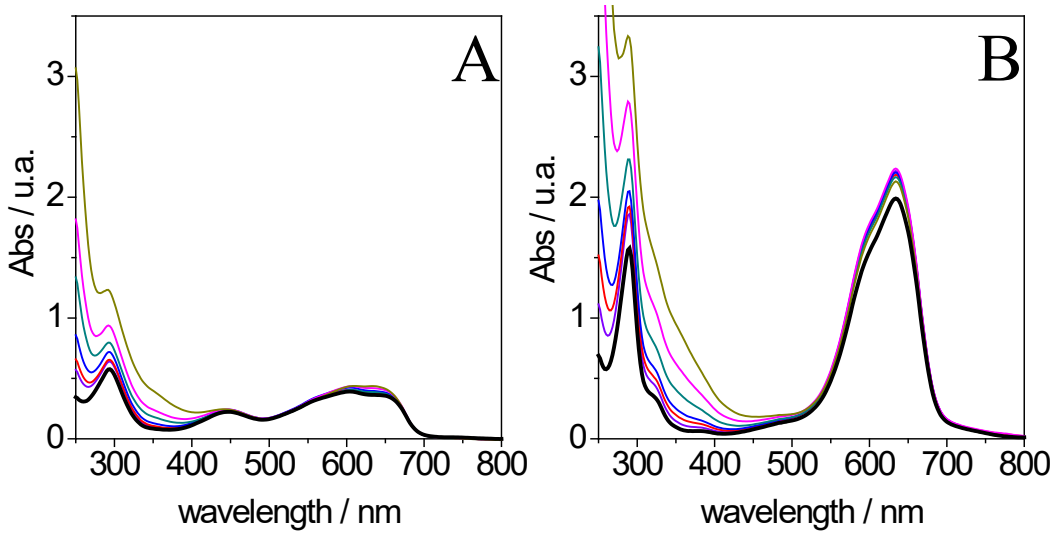

Figure 3.

This manuscript version is made available under the CC-BY-NC-ND 4.0 license http://creativecommons.org/licenses/by-nc-nd/4.0/

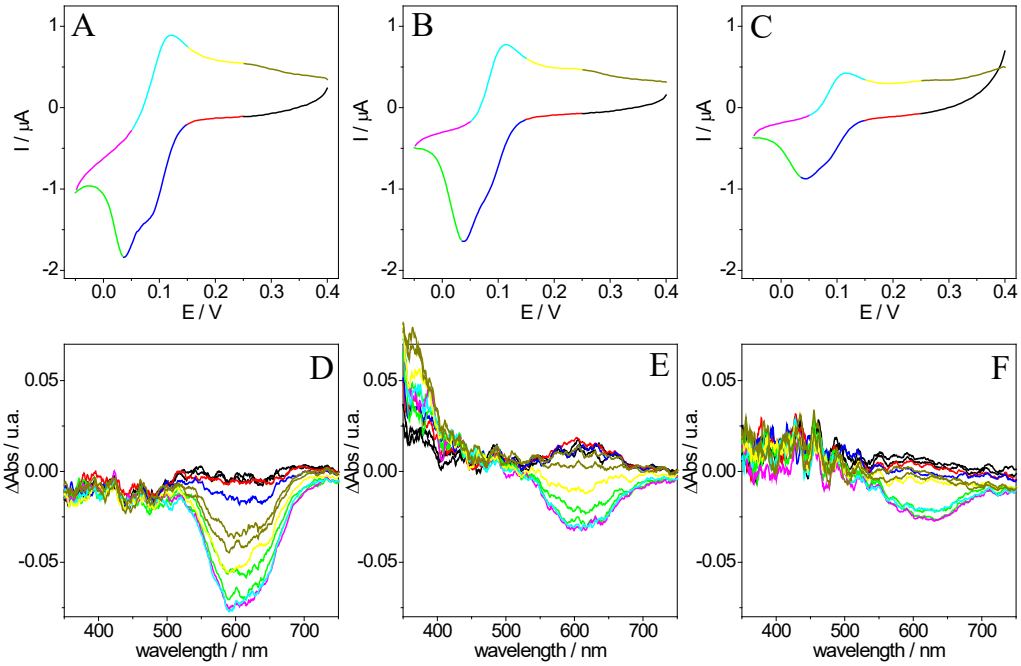

Figure 4.

This manuscript version is made available under the CC-BY-NC-ND 4.0 license http://creativecommons.org/licenses/by-nc-nd/4.0/

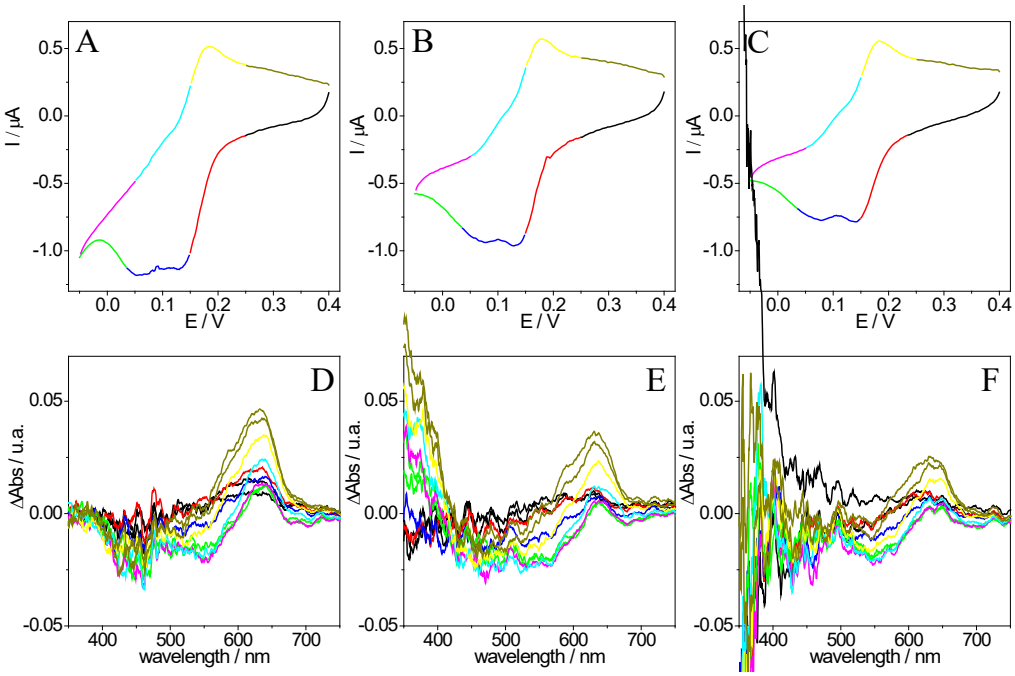

Figure 5

This manuscript version is made available under the CC-BY-NC-ND 4.0 license http://creativecommons.org/licenses/by-nc-nd/4.0/

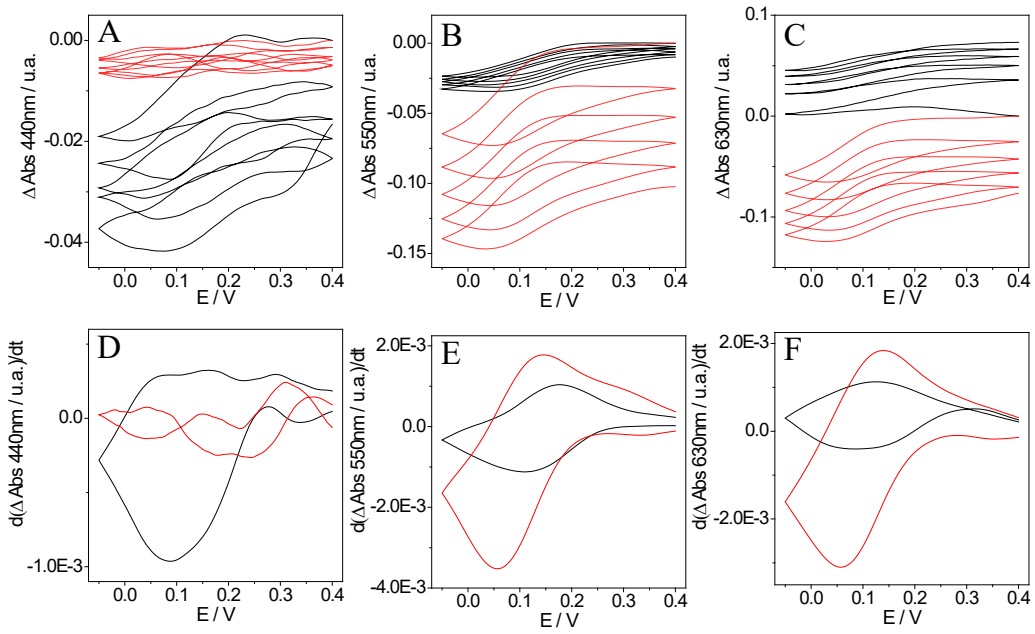

Figure 6

This manuscript version is made available under the CC-BY-NC-ND 4.0 license http://creativecommons.org/licenses/by-nc-nd/4.0/

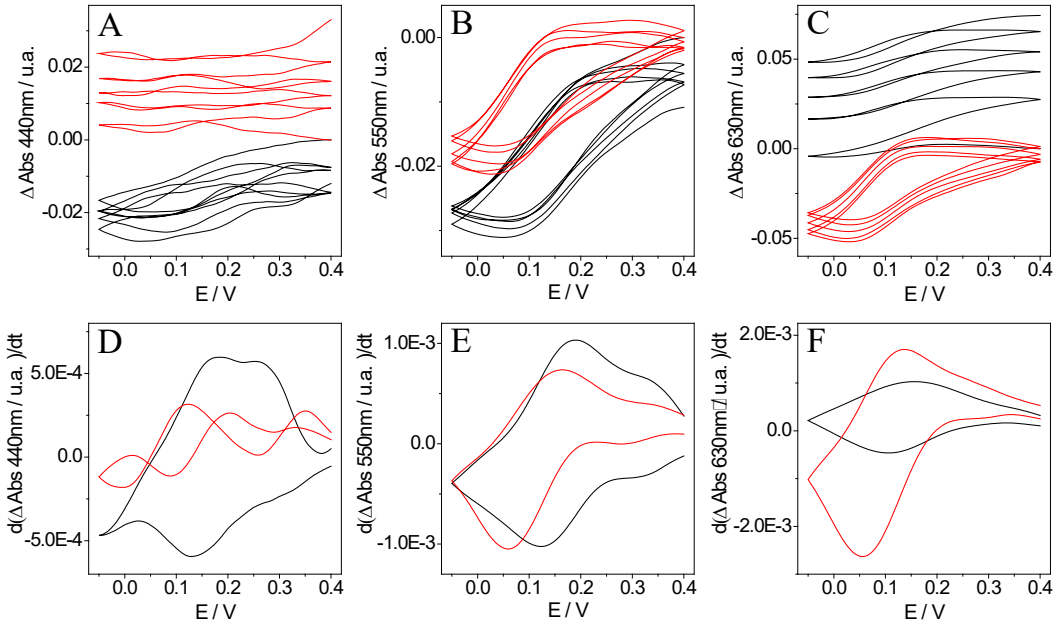

Figure 7.

This manuscript version is made available under the CC-BY-NC-ND 4.0 license http://creativecommons.org/licenses/by-nc-nd/4.0/